5-Aminosalicylic acid attenuates paraquat-induced lung fibroblast activation and pulmonary fibrosis of rats

HUI CHEN[1*], JINFENG CUI[2*], JUAN WANG[2], YUAN WANG[2], FEI TONG[2], YINGPING TIAN[2], YU GONG[2], YU MA[2], LIANG LIU[2] and XIANGHONG ZHANG[2,3]

[1]Emergency Department; [2]Department of Pathology, The Second Hospital, Hebei Medical University; [3]Laboratory of Pathology, Hebei Medical University, Shijiazhuang, Hebei 050000, P.R. China

Received February 18, 2021; Accepted October 18, 2021

DOI: 10.3892/mmr.2021.12574

Abstract. Pulmonary fibrosis is one of the most important pathological processes associated with paraquat (PQ) poisoning. 5-Aminosalicylic acid (5-ASA) has been shown to be a promising agent against fibrotic diseases. In the present study, the alleviating role of 5-ASA was evaluated in a rat model of pulmonary fibrosis induced by PQ intragastric poisoning (80 mg/kg). Wistar rats were divided into control, PQ, 5-ASA (30 mg/kg daily, 14 days) and PQ + 5-ASA groups. Histological examination revealed congestion, edema and inflammatory cell infiltration in the bronchial and alveolar walls at 3 days after PQ exposure. Alveolar septum thickening with alveolar lumen narrowing was observed at 14 days, while fibroblast proliferation, increase in collagen fiber number and fibrous thickening of the alveolar walls were observed at 28 day. All the aforementioned pulmonary injury changes in the PQ group were attenuated in the PQ + 5-ASA group. Hydroxyproline (HYP) content increased in the lung tissues of the rats at 14 days after PQ treatment and reached a peak at 28 days. Compared with the PQ group, HYP contents of lung tissue decreased at 14 and 28 days after PQ + 5-ASA treatment. Masson's trichrome staining revealed that the increase in the amount of collagen fibers in the lung tissues of rats in the PQ group was inhibited by 5-ASA treatment, further confirming the alleviating effect of 5-ASA on fibrosis. In addition, the results showed that 5-ASA attenuated the upregulation of transforming growth factor-β1 and phosphorylated-SMAD3, and the reduction of peroxisome proliferator activated receptor γ induced by PQ in lung tissue of rats and human lung fibroblast WI-38 VA13 cells. In conclusion, the results suggested that 5-ASA had an alleviating effect on PQ-induced pulmonary fibrosis, partly by suppressing the activation of the TGF-β1 signaling pathway.

Correspondence to: Professor Xianghong Zhang, Department of Pathology, The Second Hospital, Hebei Medical University, 215 Heping Western Road, Shijiazhuang, Hebei 050000, P.R. China
E-mail: zhangxianghong2008@163.com

*Contributed equally

Key words: 5-Aminosalicylic acid, paraquat, peroxisome proliferator activated receptor γ, pulmonary fibrosis, transforming growth factor-β/Smad3

Introduction

As an effective herbicide, paraquat (PQ, 1,1-dimethyl-4,4-bipyridinium) is a highly toxic pro-oxidant that is widely used worldwide (1). To date, human PQ intoxication due to accidental exposure or suicide intention has been observed (2). PQ poisoning induces multi-organ failure involving lung, gastrointestinal tract, pancreas, kidney, liver, heart and brain injury (3). Pulmonary fibrosis is the most typical feature of PQ poisoning and continues for several days to weeks after PQ ingestion (4). Although the underlying mechanism of PQ-induced pulmonary fibrosis remains unclear, inflammation, oxidative stress, epithelial-to-mesenchymal transition (EMT) and fibrogenic pathways, such as transforming growth factor (TGF)-β/SMAD and PI3K/Akt/mTOR signaling pathways can be involved in the pathogenesis of pulmonary fibrosis induced by PQ (1,5). TGF-β1 is considered a 'master switch' in the fibrosis process. Kan *et al* (6) observed that TGF-β1 expression was elevated in the serum and lung tissues of rats exposed to PQ. Han *et al* (7) demonstrated that the TGF-β/SMAD pathway was an important process in the development of PQ-induced pulmonary fibrosis. Recent studies have focused on the TGF-β/SMAD pathway as an important target for drugs such as doxycycline and tacrolimus to attenuate PQ-induced pulmonary fibrosis (8,9).

TGF-β1 has been reported to be the key growth factor that initiates tissue repair, and its sustained production is involved in the development of tissue fibrosis (7). TGF-β1 activates the downstream transcription factor SMAD and triggers the intracellular signaling pathway (10). An early study by Sato *et al* (11) showed that targeted disruption of TGF-β1/SMAD3 signaling protected against renal tubulointerstitial fibrosis induced by unilateral ureteral obstruction in mice lacking SMAD3 (SMAD3 ex8/ex8). Several other studies using different models of kidney disease further confirmed the central role of the SMAD3 pathway in the pathogenesis of interstitial fibrosis (12,13). The peroxisome proliferator activated receptor γ (PPARγ) is well-known for its ability to regulate glucose and lipid metabolism. The interaction between TGF-β1 and PPARγ is involved in the

development of fibrosis. TGF-β1 controls PPARγ expression, transcriptional potential and activity partly through SMAD3 signaling in murine lung fibroblasts (14). PPARγ is an inhibitory regulator of the TGF-β1/SMAD pathway, while TGF-β1 induces fibrosis-related genes that suppress PPARγ. PPARγ is an important regulator of TGF-β1-associated diseases, such as pulmonary arterial hypertension, parenchymal lung diseases and Marfan's syndrome (15).

5-Aminosalicylic acid (5-ASA) is an anti-inflammatory agent. Over the past decades, 5-ASA preparations have been specific and first-line therapeutic drugs for mild to moderate active inflammatory bowel disease (IBD) (16). As a PPAR-γ agonist, 5-ASA is a widely used first-line medication for the treatment of ulcerative colitis (17). Activation of PPAR-γ signaling plays an important role in alleviating the effects of 5-ASA on colitis (18). Tissue damage and inflammation are important triggers for regeneration and fibrosis. PPAR-γ has been demonstrated not only to be able to downregulate pro-inflammatory cytokine production, such as interleukin (IL)-4, -5 and -6, but also to interfere with profibrotic molecules, including platelet-derived growth factor, IL-1 and TGF-β, the main promoters of fibrosis (19). Moreover, 5-ASA was found to reduce TGF-β signaling, as indicated by the reduction in TGF-β-specific reporter gene activity (20). The intestinal anti-inflammatory effect of 5-ASA is dependent on PPARγ (18,21), and its anti-neoplastic effect in the intestine is also mediated by PPARγ (20). Thus, it is clear that PPARγ is the key mediator of the anti-inflammatory and antineoplastic effects of 5-ASA. As PPARγ is also involved in the development of fibrotic diseases, there is interest in determining whether 5-ASA could play a role in the interaction of PPARγ and the TGF-β1/SMAD3 pathway in the pathogenesis of pulmonary fibrosis, and whether it could be used as a potential drug for PQ poisoning. As pulmonary fibrosis is the most typical feature of PQ poisoning, whether the agonist of PPAR-γ, 5-ASA, may be used as a potential drug for alleviating pulmonary fibrosis induced by PQ is worthy of investigation.

To date, to the best of our knowledge, there have been no reports on the clinical use of 5-ASA in the treatment of human PQ poisoning; however, experimental studies in animals have been performed. Wang *et al* (22) found that 5-ASA could attenuate PQ-induced acute renal injury damage by activating the Nrf2-antioxidant response element signaling pathway. A recent study by Ramadan *et al* (23) revealed that mesalazine, with 5-ASA as its main ingredient, had potential as a novel anti-fibrotic agent by reducing oxidative damage and altering the TNF-α pathway as an anti-inflammatory drug, which was demonstrated by its ability to downregulate TGF-β1, osteopontin, α-SMA and caspase-3 signaling pathways in liver fibrosis in rats (23). A previous study by Hoffmann *et al* (24) also provided experimental pre-clinical evidence for the antifibrotic effects of mesalazine in an *in vitro* model of cardiac fibrosis.

Therefore, the aim of the present study was to explore the effects of 5-ASA on pulmonary fibrosis progression in a PQ intoxication rat model. It was first investigated whether 5-ASA exerted protective effects against PQ-induced pulmonary fibrosis. Following which, the putative mechanism of action of 5-ASA in preventing PQ-induced pulmonary fibrosis was explored. This study provided insights for the treatment of PQ poisoning.

Materials and methods

Reagents. PQ (33.5%) was purchased from Syngenta Nantong Crop Protection Co., Ltd. 5-ASA (98.5%, chemical purity) was purchased from J&K Scientific Ltd. The primary antibodies used were as follows: Rabbit anti-human PPARγ (cat. no. P37231; Bioworld Technology, Inc.), rabbit anti-human TGF-β1 antibodies (cat. no. P01137; Bioworld Technology, Inc.), rabbit anti-human SMAD3 (cat. no. AF6362; Affinity Biosciences, Ltd.), rabbit anti-human phosphorylated (p)-SMAD3 antibody (cat. no. AF3362; Affinity Biosciences, Ltd.) and mouse anti-human β-actin monoclonal antibody (cat. no. sc-47778; Santa Cruz Biotechnology, Inc.).

Animals. In this study, 100 healthy male Wistar rats aged 6-8 weeks and weighing 180-220 g were purchased from the Animal Center of Hebei Medical University (Shijiazhuang, China). The animals were placed in a ventilated room at 22±2˚C with a 12 h light/dark cycle, with *ad libitum* access to food and water. All animal experiments conformed to the guidelines of the Ethics Committee for Laboratory Animals of Hebei Medical University. All experiments were performed in compliance with the Guide for the Care and Use of Laboratory Animals of the National Institutes of Health (25) and were reviewed and approved by the Ethics Committee for the Use of Experimental Animals at Hebei Medical University (approval no. 1608303).

Animal models and tissue sampling. The Wistar rats were randomly divided into four groups, with 25 rats in each group: i) Control; ii) PQ; iii) 5-ASA and iv) PQ + 5-ASA. The concentration of PQ in this study was selected based on the results of our preliminary experiments and related literature (26,27). On the first day, the rats in the PQ and PQ + 5-ASA groups were administered doses of 80 mg/kg PQ by gavage, whereas, in the control and 5-ASA groups, the rats were treated with distilled water, and 2 h later, equal amounts of distilled water were administered to the control and PQ groups, while 30 mg/kg 5-ASA in distilled water was intragastrically administered to the 5-ASA and PQ + 5-ASA groups. On the second day, only equal amounts of distilled water were administered to the control and PQ groups. At the same time, 30 mg/kg 5-ASA was administered to the 5-ASA and PQ + 5-ASA groups and the steps of the second day were repeated once a day for up to 14 days. Rats were sacrificed by cervical dislocation after anesthesia by intraperitoneal injection of a saturated pentobarbital sodium solution (40 mg/kg) at 3, 14 and 28 days after PQ administration. General pathological changes in the rats in each group were observed, including size, congestion and dot bleeding. To distinguish the rats' left and right lungs, each left lung was placed in a frozen pipette and stored in a -70˚C liquid nitrogen freezer to detect hydroxyproline (HYP). The right lung was immersed in 10% formalin and embedded in paraffin.

Comparison of relative weight. Before the rats were sacrificed, the rats were weighed and the ratio of the weight at day 3, 14 and 28 to the weight of the rats on the first day, that is, the relative weight, was calculated.

Lung coefficient. The whole lung and trachea of the rats were collected, the trachea was cut between the 5 and 6 cartilage rings above the tracheal bifurcation, clean filter paper was used to absorb the blood and tissue fluid on the lung surface, and it was weighed with a high-precision balance. The pulmonary coefficient was calculated as follows: Lung coefficient (LI)= total lung wet weight (mg)/body weight (g) x100%.

Histopathological examination. The right lung tissue samples were fixed in 10% formalin at room temperature for 4-6 h, embedded in paraffin and sectioned (thickness of 5 μm). The slides were subsequently stained with hematoxylin solution at room temperature for 5 min followed by five immersions in 1% acid ethanol (1% HCl in 70% ethanol) and then rinsed in distilled water. Then, the sections were stained at room temperature with eosin solution for 3 min, followed by dehydration with graded alcohol and washing in xylene. The slides were then examined under a light microscope (RM2245; Leica Microsystems GmbH) by an experienced pathologist who was blinded to the treatment received by each animal.

Masson's trichrome staining. The slides were deparaffinized and subjected to Masson staining to detect fibrosis. Briefly, the tissue sections (thickness, 5 μm) were cut and placed on standard microscopy slides. After deparaffinization and rehydration, the slides were immersed in Bouin's solution (cat. no. HT10132; Sigma-Aldrich; Merck KGaA) at 56˚C for 15 min. Subsequently, the slides were washed with tap water for 5 min. Next, the sections were stained in Weigert's hematoxylin for 5 min at room temperature and then washed again with tap water for 5 min and rinsed in distilled water. Next, the slides were stained in Biebrich scarlet-acid fuchsin for 5 min at room temperature, rinsed in distilled water, incubated in phosphotungstic-phosphomolybdic acid for 5 min at room temperature, dyed with aniline blue for 5 min at room temperature and fixed in 1% acetic acid for 2 min at room temperature. Finally, the slides were rinsed in distilled water, dehydrated and mounted in synthetic resin. Slides stained with Masson's trichrome stain were observed using the Leica microscope. The smooth muscle cell cytoplasm was stained red, while the collagenous fibrous tissue was stained blue.

Pathology scores were assessed using the method described by Szapiel *et al* (28). The pathological score consisted of alveolar inflammation and pulmonary fibrosis scores. The criteria for alveolitis were as follows: i) Grade 0, normal alveolar morphology, no alveolar inflammation; ii) grade I, mild alveolitis, alveolar septum widened by inflammatory cell infiltration; iii) grade II, moderate alveolitis; and iv) grade III, severe alveolitis, a large number of infiltrating inflammatory cells and diffusely distributed lesions. The criteria for pulmonary fibrosis were as follows: i) Grade 0, normal lung tissue, with few or no filamentous collagen fibers; ii) grade I, slight increase in collagen fiber amount, with thin bundle morphology; iii) grade II, moderate increase in collagen fiber amount fused into fine bands, with alveolar structure disorder; and iv) grade III, substantial increase in collagen fiber amount into a broadband or flaky morphology, with alveolar collapse and fusion, as well as structural disorder. Alveolar inflammation and pulmonary fibrosis scores were 0 points for grade 0, 2 points for grade I, 3 points for grade II and 4 points for grade III; these scores were used for statistical analysis.

Determination of HYP. According to the manufacturer's instructions for the Hydroxyproline Assay kit (cat. no. BC0250; Beijing Solarbio Science & Technology Co., Ltd.), lung tissues were isolated to determine the optical density (OD) of the samples at a wavelength of 550 nm using a microplate reader (Thermo Fisher Scientific, Inc.) and the level of HYP was calculated accordingly.

Cell culture and treatment. Human lung fibroblasts WI-38 VA13 purchased from American Type Culture Collection were grown in DMEM/F12 (Gibco; Thermo Fisher Scientific, Inc.) at 37˚C supplemented with 10% fetal bovine serum (FBS; Gibco; Thermo Fisher Scientific, Inc.) and 100 U/ml penicillin and streptomycin in 5% CO_2/95% air. When the cells reached 80% confluence, they were randomly divided into four groups: i) Control; ii) PQ; iii) 5-ASA; and iv) PQ + 5-ASA groups. The cells were incubated with 200 μM of PQ for 12, 24 and 48 h, with or without pretreatment with 5-ASA (10 mM) at 37˚C for 2 h. Cells were collected at 12, 24 and 48 h after PQ treatment.

Western blotting. After treatment, cells were washed with ice-cold PBS. Total cell proteins were extracted using lysis buffer (1% Triton X-100, 150 mM NaCl, 2 mM EDTA, 50 mM Tris-HCl, 10% phosphatase inhibitors and 1% cocktail). Total protein concentration was quantified using the Bradford Protein Assay Kit (Bio-Rad Laboratories, Inc.). A total of 40 μg protein/lane protein was separated via 10% SDS-PAGE and then transferred to a PVDF membrane. Subsequently, the membranes were blocked with 5% skimmed milk with PBS with 0.05% Tween-20 for 1 h at room temperature and then incubated overnight at 4˚C with specific primary antibodies at a 1:1,000 dilution in blocking solution. After washing, the membranes were incubated with horseradish peroxidase-conjugated goat anti-rabbit IgG secondary antibody (cat. no. sc-2030; Santa Cruz Biotechnology, Inc.) at a 1:5,000 dilution for 1 h at room temperature and visualized using an ECL chemiluminescent detection system (Santa Cruz Biotechnology, Inc.). Band density was semi-quantified using GeneTools Image Analysis Software (version 4.02; Syngene Europe) and normalized to β-actin.

Immunohistochemical (IHC) staining. Tissues were fixed in 10% neutralized formalin for 48 h at room temperature and embedded in paraffin blocks. Sections (4-μm thick) were prepared from paraffin blocks. After deparaffinization, antigen retrieval was performed in 10 mmol/l of citrate buffer at room temperature for 15 min. Endogenous peroxidase activity was blocked with 3% hydrogen peroxide in methanol for 10 min at room temperature. Blocking was carried out at room temperature for 1 h using 10% normal goat serum (Vector Laboratories, Ltd.). Incubation with primary antibodies against TGF-β (1:100) and PPARγ (1:100) was conducted overnight at 4˚C in a humidified chamber and then washed with PBS. Subsequently, sections were incubated in PBS with Tween-20 (0.5%) containing a biotin-conjugated secondary antibody (cat. no. bs-0346R-Bio; BIOSS) at 1:200 dilution for 1 h at room temperature and 3,3'diaminoenzidine was used to locate the specific antigens in each section. Slides were counterstained with hematoxylin for 30 sec at room temperature (29). The primary antibody was replaced with PBS as a negative control.

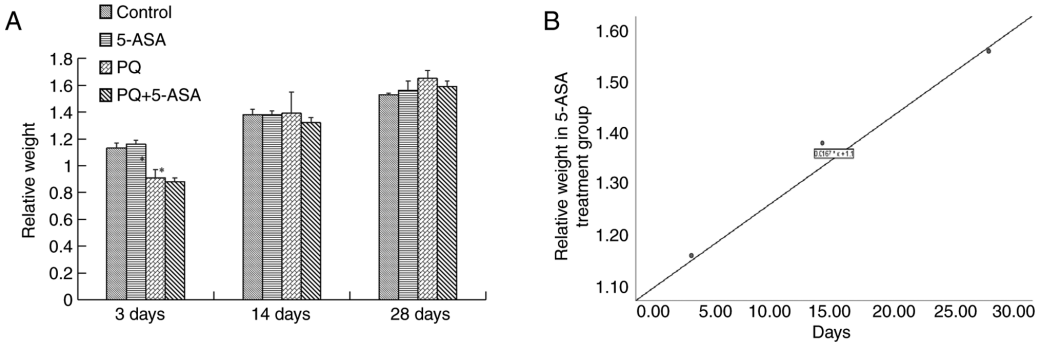

Figure 1. A PQ-induced decrease in relative body weight is improved by 5-ASA. (A) Relative weight changes of rats in different groups. (B) Relative body weight gradually increased with time in 5-ASA group (r=0.992). The time-effect relationship was analyzed using Pearson's correlation analysis. Data are presented as the mean ± SD. *P<0.05 vs. control group. 5-ASA, 5-aminosalicylic acid; PQ, paraquat.

All slides were scored by an experienced pathologist. Images were captured using an Olympus AH2 Vanox Microscope System (light microscope; Olympus Corporation).

The levels of TGF-β1 and PPARγ are described based on the ratio of positive cells to the intensity of the reaction. The parameter was classified and a combined score was used to determine positive or negative results according to previously defined criteria (30). For the score of positive cell ratio, 0-1, 1-10, 10-50, 50-80 and 80-100% were scored as 0, 1, 2, 3 and 4, respectively. For the intensity score, negative, weakly positive, positive and strongly positive were scored as 0, 1, 2 and 3, respectively. IHC score=positive cell ratio score x intensity score.

Statistical analysis. Statistical analysis was performed using one-way analysis of variance (ANOVA) with SPSS 16.0 (SPSS, Inc.). One-way ANOVA followed by the Tukey's post-hoc test was used to compare differences between groups. The time-effect relationship was analyzed using Pearson's correlation analysis. All results were confirmed using at least three independent experiments. The results are presented as the mean ± standard deviation. P<0.05 was considered to indicate a statistically significant difference.

Results

Rat general conditions after PQ exposure. In the PQ group, the rats displayed a series of symptoms, including sluggishness, lethargy, irritability and bloody discharge in the mouth, nose and eyes 2 h after PQ exposure. The poisoning symptoms progressively worsened from 3 to 28 days after PQ exposure, including dyspnea, abdominal breathing and perioral cyanosis in the respiratory system, diarrhea in the alimentary system and oliguria, anuresis and hematuria in the urinary system. The poisoning manifestations, both general and systemic, were alleviated in the PQ + 5-ASA group (data not shown).

Relative body weight gradually increased with time in the 5-ASA group (r=0.992). It showed no changes compared with the control group. After PQ exposure, the relative weight decreased to a minimum at 3 days and gradually increased to the control level at 14 days. In the PQ + 5-ASA group, the relative body weight decreased to a minimum at 3 days. The body weight decrease was statistically significant when compared with the control group and 5-ASA group at 3 days (Fig. 1A and B). Therefore, the PQ-induced decrease in relative body weight could be improved by 5-ASA.

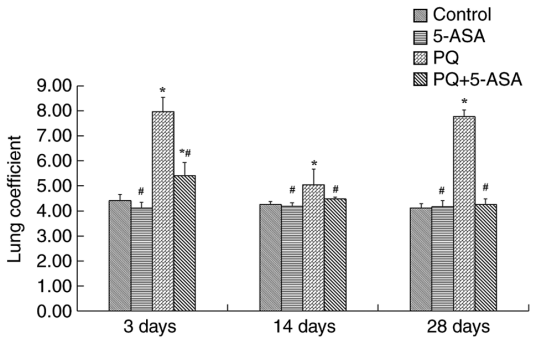

Figure 2. Lung coefficient changes of rats in different groups. Data are presented as the mean ± SD. *P<0.05 vs. control group; #P<0.05 vs. PQ group. 5-ASA, 5-Aminosalicylic acid; PQ, paraquat.

5-ASA attenuates PQ-induced pulmonary damage. The lungs in the control and 5-ASA groups were normal in size and pink in color, while lungs in the PQ group notably increased in size and congestion and dot bleeding could be seen within 14 days after PQ exposure, turning grayish with uneven surface 28 days after PQ exposure (data not shown). The changes in the lungs in the PQ + 5-ASA group were markedly alleviated; no obvious bleeding was observed and the lung surface was smooth.

There was no significant difference in lung coefficient between the 5-ASA group and control group. After PQ exposure, the lung coefficient increased significantly, reached a peak on day 3, decreased on day 14 compared with the 3 days, but increased again on day 28, showing a biphasic increase. The lung coefficient in each time period in the PQ group was significantly higher compared with the control group. Compared with the control group, the lung coefficient of the PQ group was significantly increased, especially at day 3. However, the lung coefficient at each time point in the PQ + 5-ASA group was significantly lower compared with the PQ group. In conclusion, lung coefficient measurements further confirmed that 5-ASA treatment could alleviate the changes caused by PQ in the lungs (Fig. 2).

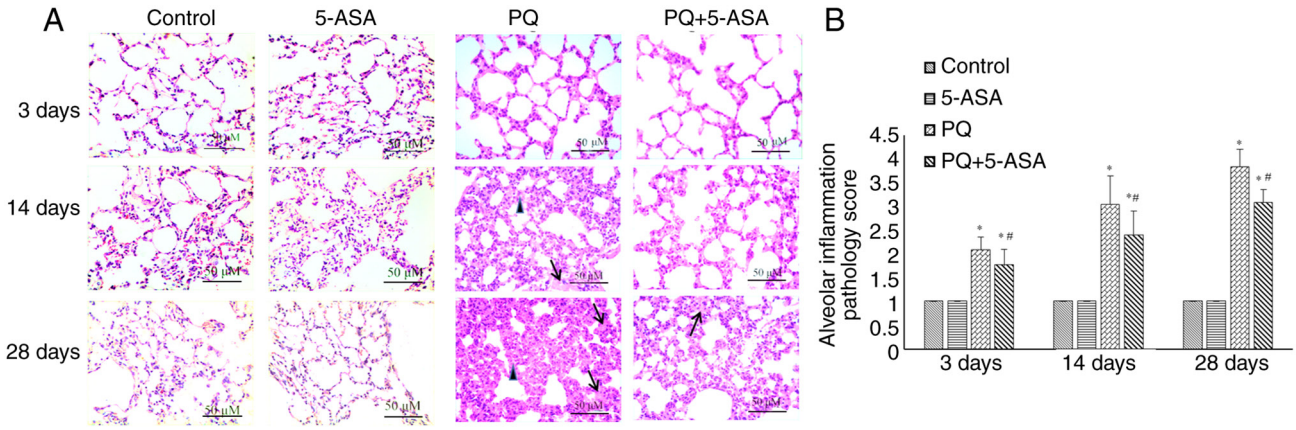

Figure 3. H&E-stained histological evaluation of rat lungs in the control, 5-ASA, PQ and PQ + 5-ASA groups at days 3, 14 and 28 after PQ intragastric administration (all groups magnification, x200). (A) Compared with the control group, the PQ group showed progressive interstitial edema and inflammatory cell infiltration in the alveolar space and septum at day 3. The PQ group at days 14 and 28 showed fibroblast proliferation, increased collagen fiber amount (black arrowhead) and fibrous thickening (black triangle) of the alveolar walls. At the same time, the PQ + 5-ASA group showed remarkably decreased pulmonary pathological damage in rats. (B) Alveolar inflammation pathology score in lung tissue. All quantitative data are presented as the mean ± SD. *P<0.05 vs. control group; #P<0.05 vs. PQ group. 5-ASA, 5-Aminosalicylic acid; PQ, paraquat.

Histologically, the morphological changes in the lungs of rats in different groups were evaluated by H&E staining (Fig. 3A). Except for a few phagocytes in the lumens of the alveoli, no changes, including edema, congestion, bleeding and inflammatory modifications, were observed in the lungs of the control and 5-ASA groups. Alveolitis was observed in the lungs of rats after PQ exposure. Congestion, edema and inflammatory cell infiltration were observed in the bronchial and alveolar walls at 3 days after PQ exposure. Alveolar septum thickening with alveolar lumen narrowing, diffuse pulmonary hemorrhage and hyaline membrane formation were observed at 14 days after PQ exposure. At the later stage, fibroblast proliferation, increased collagen fiber amount and fibrous thickening of the alveolar walls was also observed at 28 days after PQ exposure. All pulmonary injury changes observed in the lungs of rats in the PQ group were notably attenuated in the PQ + 5-ASA groups, as evidenced by a decrease in the degree of congestion, inflammatory cell infiltration, bleeding at an early stage (<14 days) and fibrous proliferation at the late stage (28 days) after PQ exposure.

5-ASA attenuates PQ-induced fibrosis in lung tissues of rats

HYP content analysis of the lung tissues. Pulmonary fibrosis is characterized by the accumulation of collagen. HYP is a non-essential amino acid found in collagen that serves a crucial role in collagen synthesis and is frequently used as a biomarker of tissue fibrosis (31). HPY content changes were measured in lung tissues in different groups. The results showed that HYP content significantly increased in the lung tissues of the rats at 14 days after PQ treatment and reached a peak at 28 days compared with the control group. Compared with the HYP changes in the PQ group, HYP content of lung tissue was significantly lower in the lung tissues of rats at 14 and 28 days after PQ + 5-ASA treatment (Fig. 4), suggesting that 5-ASA treatment could significantly alleviate the degree of collagen accumulation induced by PQ.

Masson's trichrome staining. Masson's trichrome staining revealed that the collagen fibers were stained blue. The results (Fig. 5A) showed that, compared with those in the control group and 5-ASA group, the amount of blue-stained collagen

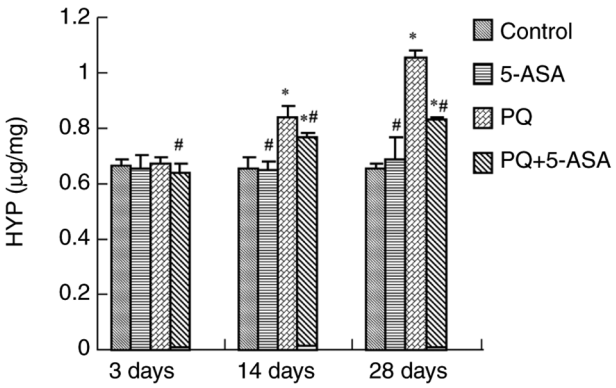

Figure 4. Effects of PQ on the HYP content in the lung tissues of rats. Compared with the PQ group, 5-ASA treatment significantly decreased the HYP content in the lung tissues of rats. All quantitative data are presented as the mean ± SD. *P<0.05 vs. control group; #P<0.05 vs. PQ group. 5-ASA, 5-Aminosalicylic acid; PQ, paraquat; HYP, hydroxyproline.

fibers in the lung tissues of rats in the PQ group increased at 14 and 28 days. Collagen fibers were mainly concentrated in the alveolar thickening area and bronchioles. With 5-ASA treatment, collagen deposition (blue staining) of lung tissue in the PQ + 5-ASA groups was lower than that in the PQ group alone, further confirming the alleviating effect of 5-ASA on the increase in collagen fiber amount induced by PQ at 14 and 28 days.

No pathological changes were found in the lungs of the rats in the control and 5-ASA groups, while injury and fibrosis changes with different severity were observed in rats of the other two groups. Further quantitative analysis showed that the inflammation score in the PQ group increased from 3 to 28 days after PQ exposure compared with the control group. Inflammation scores at all time points (3, 14 and 28 days) in the PQ + 5-ASA groups all decreased compared with those in the PQ group, suggesting that 5-ASA treatment could partly alleviate the degree of inflammation induced by PQ (Fig. 3B). The fibrosis score increased at 14 and 28 days after PQ exposure compared with the control group, while that in the PQ +

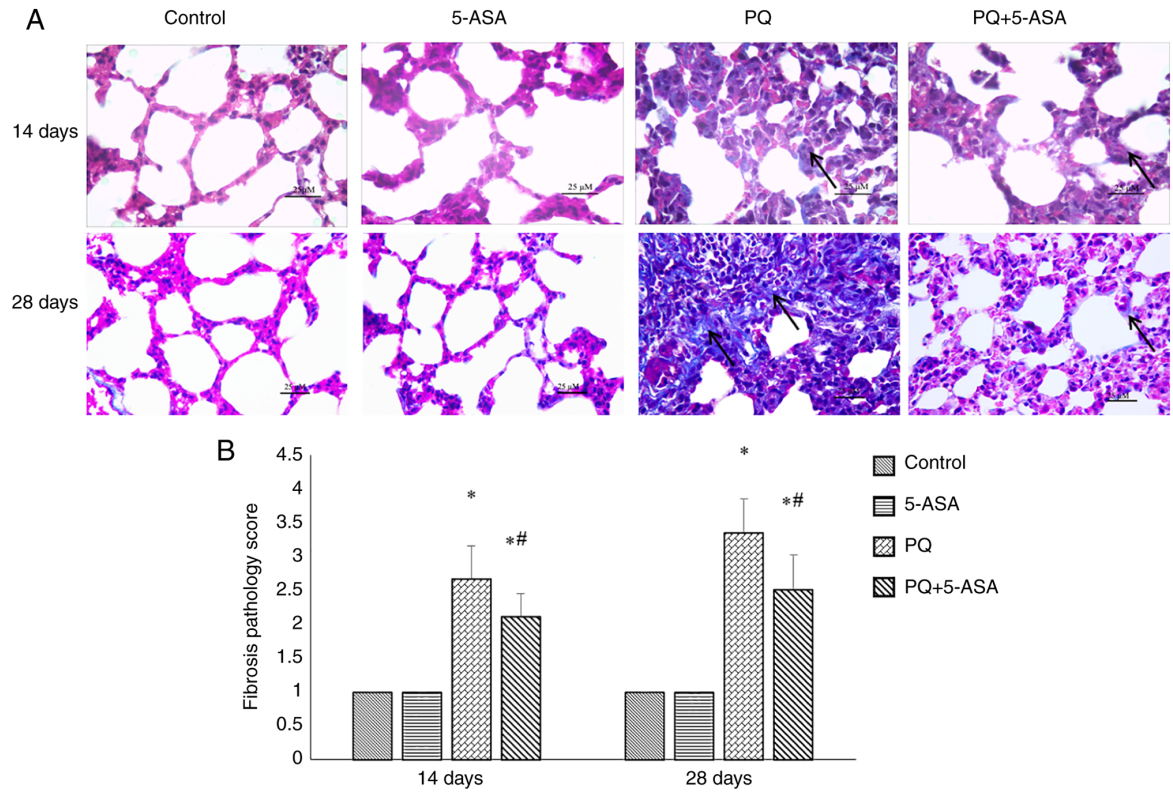

Figure 5. Histological evaluation of rat lungs in the control, 5-ASA, PQ and PQ + 5-ASA group on days 14 and 28 after PQ exposure with Masson's stain. (A) Compared with the control group, PQ exposure increased fibrosis (seen as blue collagen deposition, black arrowhead) in the alveolar regions and small bronchioles at days 14 and 28. The PQ + 5-ASA group exhibited decreased collagen deposition in the lung tissues of rats. Magnification, x400. (B) Fibrosis pathology score in lung tissue. All quantitative data are presented as the mean ± SD. *P<0.05 vs. control group; #P<0.05 vs. PQ group. 5-ASA, 5-Aminosalicylic acid; PQ, paraquat.

5-ASA group significantly decreased compared with the PQ group, suggesting that 5-ASA treatment could partly alleviate the degree of fibrosis induced by PQ (Fig. 5B).

5-ASA attenuates the upregulation of TGF-β1 and p-SMAD3 and the reduction of PPARγ induced by PQ in the lung tissue of rats in vivo and human lung fibroblasts WI-38 VA13 cells in vitro. The expression of fibrosis-related factors in the lung tissue of rats were further evaluated by IHC staining to explore the putative anti-fibrotic mechanism of 5-ASA. The IHC staining results showed that TGF-β1 expression increased from days 3 to 28 after PQ exposure compared with the control group. Compared with that in the PQ group, the expression level of TGF-β1 decreased in the PQ + 5-ASA group at each time point (Fig. 6A and B). The expression of PPARγ in the lung tissue of rats in the PQ group obviously decreased compared with that in the control group. This downregulation of PPARγ induced by PQ could be partly inhibited by 5-ASA treatment in the lung tissue of rats (Fig. 7A and B). In addition, the activation of SMAD3, which is another key member in the TGF-β1/SMAD3 pathway, was further analyzed. The active form of SMAD3, p-SMAD3 was determined by western blotting. The results showed that PQ exposure significantly increased p-SMAD3 expression in lung tissues compared with that in the control group at each time point. The p-SMAD3 level was significantly downregulated in the lung tissue of PQ + 5-ASA-treated rats compared with that in the PQ treatment group (Fig. 8A and C). PQ treatment had no significant effects on regulating the protein levels of SMAD3 (Fig. 8B and D). Furthermore, the p-SMAD3/total SMAD3 ratio was significantly downregulated in the lung tissue of PQ + 5-ASA-treated rats compared with that in the PQ treatment group (Fig. 8E).

Studies have shown that myofibroblast proliferation in the lung tissue of patients is the basis for pulmonary fibrosis (32,33). Based on the aforementioned results, the effect of 5-ASA on the TGF-β1 pathway after PQ exposure was further explored in human lung fibroblasts WI-38 VA13 cells *in vitro*. The results, as determined by western blotting, were consistent with those *in vivo* and revealed that pretreatment with 5-ASA significantly reversed the reduction of PPARγ (Fig. 9A) and the increase in TGF-β1 (Fig. 9B) and p-SMAD3 (Fig. 9C) levels induced by PQ. PQ treatment had no significant effects on regulating the protein levels of SMAD3 (Fig. 9D). Furthermore, the p-SMAD3/total SMAD3 ratio was significantly downregulated in the PQ + 5-ASA group compared with that in the PQ treatment group (Fig. 9D).

Discussion

Pulmonary fibrosis is an irreversible stage of the pathological development of PQ poisoning, leading to high mortality (34). No safe and effective treatment has been found to reverse the fibrosis process. In the present study, it was found that intragastric administration of PQ induced significant injury and fibrotic changes in the lungs of experimental rats, including congestion, edema, hemorrhage, increased lung coefficient, increased HYP

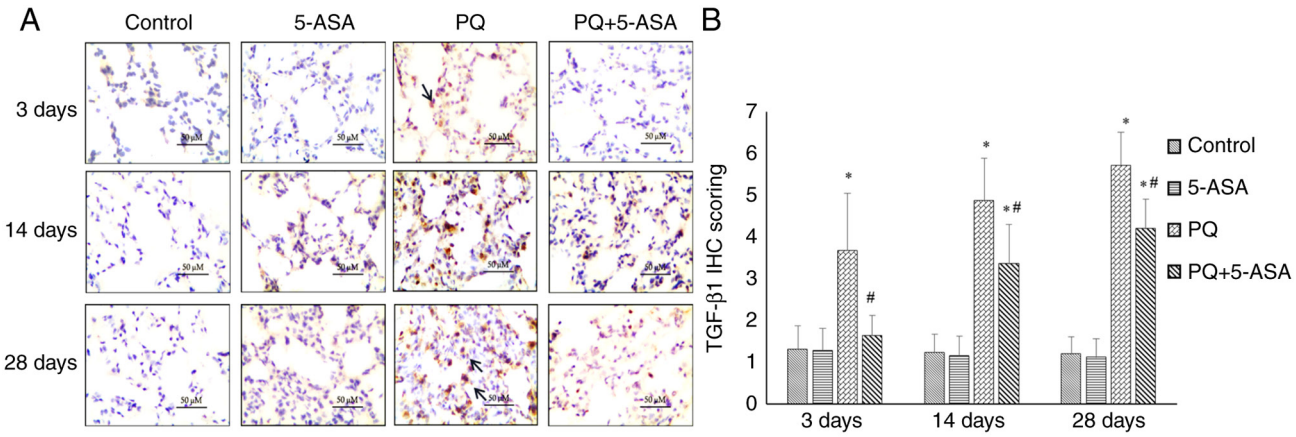

Figure 6. Treatment with 5-ASA decreases PQ-induced expression of TGF-β1 in lung tissue of rats. (A) The staining of TGF-β1 (brown in the cytoplasm, black arrowhead) was markedly downregulated by PQ + 5-ASA treatment for 14 and 28 days after PQ administration. Magnification, x200. (B) TGF-β1 IHC scores for all groups. All quantitative data are presented as the mean ± SD. *P<0.05 vs. control group; #P<0.05 vs. PQ group. 5-ASA, 5-Aminosalicylic acid; PQ, paraquat; TGF-β1, transforming growth factor β1; IHC, immunohistochemistry.

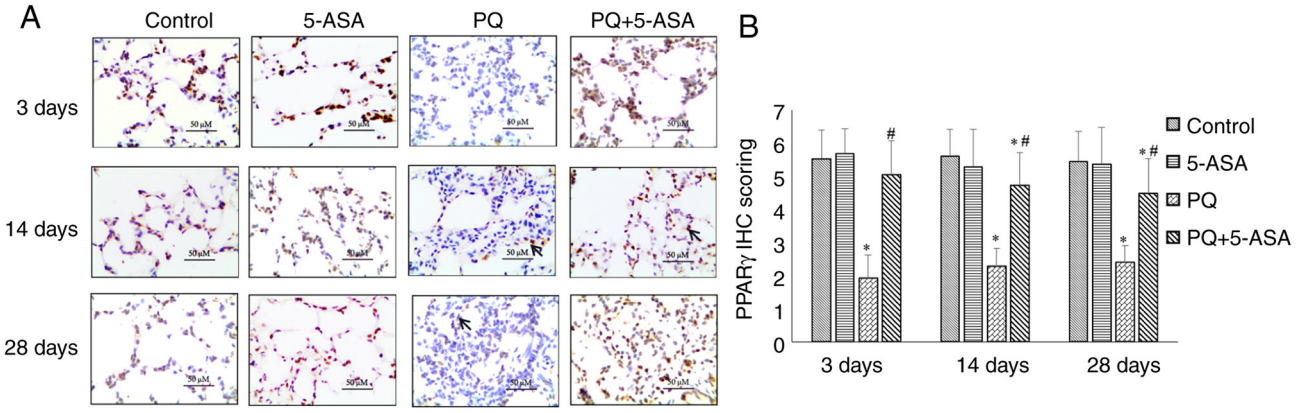

Figure 7. Treatment with 5-ASA increases PQ-induced expression of PPARγ in lung tissue of rats. (A) The staining of PPARγ (brown in the cell nucleus, black arrowhead) was markedly upregulated by PQ + 5-ASA treatment for 3, 14 and 28 days after PQ intoxication. Magnification, x200. (B) PPARγ IHC scores for all groups. All quantitative data are presented as the mean ± SD. *P<0.05 vs. control group; #P<0.05 vs. PQ group. 5-ASA, 5-Aminosalicylic acid; PQ, paraquat; PPARγ, peroxisome proliferator activated receptor γ; IHC, immunohistochemistry.

content, accumulation of collagen, increase in the amount of collagen fibers and fibrous thickening of the alveolar walls. 5-ASA treatment notably alleviated the pulmonary injury and fibrotic changes induced by PQ in rats, as evidenced by decrease in the degree of congestion, inflammatory cell infiltration, hemorrhage, lung coefficient, collagen accumulation and collagen fiber amount. Thus, this study confirmed that 5-ASA could markedly attenuate the injury and fibrotic changes induced by PQ, suggesting that 5-ASA could be used in the alleviation of pulmonary fibrosis in PQ poisoning.

TGF-β1 plays a crucial role in the induction of fibrosis. TGF-β1 signaling exerts its biological effects via the TGF-β1/SMAD/Snail signaling pathway, serving an important pathogenic role in several fibrotic diseases, such as pulmonary fibrosis and cardiac fibrosis (13,35). In the current study, the upregulation of TGF-β1 and SMAD3 activation was confirmed by observing the increased p-SMAD3 levels after PQ exposure, suggesting that the TGF-β1/SMAD signaling pathway was involved in the fibrotic changes induced by PQ. These results were in accordance with those reported in the literature on tissue fibrosis (36).

PPARs are recognized as versatile members of the ligand-activated nuclear hormone receptor superfamily of transcription factors, including steroids, thyroid hormone, retinoic acid and vitamin D (37). There are three subtypes of PPARs: PPARα, PPARβ/δ and PPARγ. Of the three PPARs identified to date, PPARγ represents the most promising PPAR target in lung diseases in view of emerging reports implicating this molecule in various pulmonary processes, for example, pulmonary thromboembolectomy, lung transplantation and severe viral pneumonia (38). Additionally, it has been reported that PPARγ activators can inhibit TGF-β1-induced myofibroblast transdifferentiation (39). In diseased tissues, PPARγ expression is inversely related to that of TGF-β1 (27). Thus, it appears that the balance between TGF-β1 and PPARγ may determine whether fibrogenesis predominates after tissue injury. In the present study, it was found that the expression of PPARγ significantly decreased in the lung tissues of rats after PQ intragastric treatment. At the same time, it was found that PQ exposure decreased the expression of PPARγ in human lung fibroblasts WI-38 VA13 cells *in vitro*. Therefore, this study suggested that PPARγ was involved in the regulation of

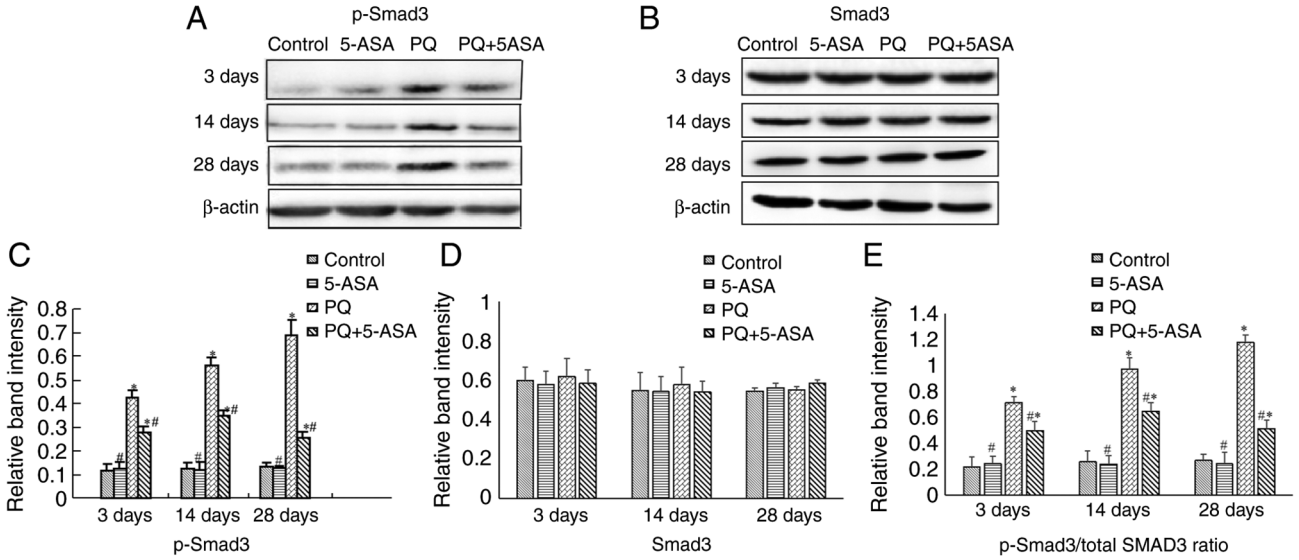

Figure 8. Level of p-SMAD3 and the expression of SMAD3 in lung tissue of rats. (A) Treatment with 5-ASA significantly decreased the level of p-SMAD3 in lung tissue of rats. (B) PQ treatment had no notable effects on regulating the protein levels of SMAD3. (C) The intensities of the immunoreactive bands of p-SMAD3 were semi-quantified using densitometric scanning. (D) The intensities of the immunoreactive bands of SMAD3 were semi-quantified using densitometric scanning. (E) p-SMAD3/total SMAD3 ratio was significantly downregulated in the lung tissue of PQ + 5-ASA-treated rats compared with that in the PQ treatment group. Values are presented as the mean ± SD. *P<0.05 vs. control group; #P<0.05 vs. PQ group. p-, phosphorylated; 5-ASA, 5-Aminosalicylic acid; PQ, paraquat.

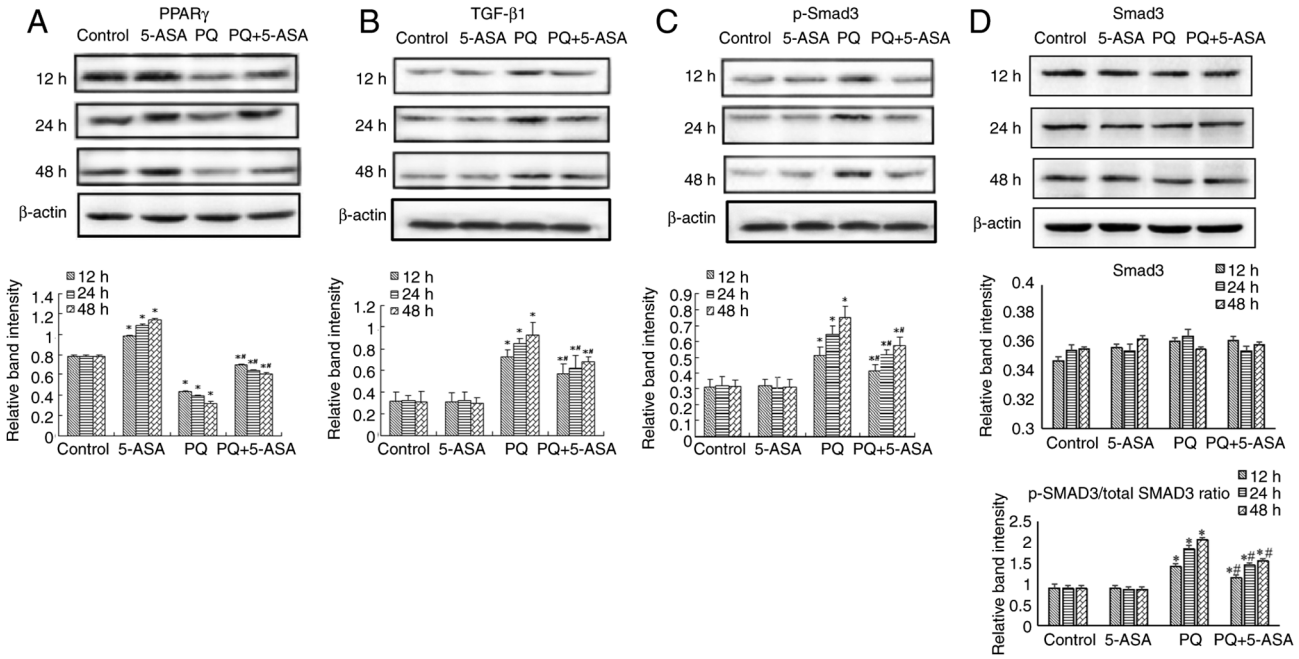

Figure 9. 5-ASA abolishes the PQ-induced activation of the TGF-β1 signaling pathway in human lung fibroblasts WI-38 VA13 cells. The WI-38 VA13 cells were pretreated with 10 mM 5-ASA for 2 h prior to treatment with 200 μM PQ for 12, 24 and 48 h. Treatment with 5-ASA (A) significantly increased the level of PPARγ and reduced the expression of (B) TGF-β1 and the (C) phosphorylation level of SMAD3 as determined by western blotting. (D) PQ treatment had no significant effects on regulating the protein levels of SMAD3. The p-SMAD3/total SMAD3 ratio was significantly downregulated in the lung tissue of PQ + 5-ASA-treated rats compared with that in the PQ treatment group. The intensities of the immunoreactive bands were semi-quantified using densiometric scanning. Values are presented as the mean ± SD. *P<0.05 vs. control group; #P<0.05 vs. PQ group. p-, phosphorylated; 5-ASA, 5-Aminosalicylic acid; PQ, paraquat; TGF-β1, transforming growth factor β1; PPARγ, peroxisome proliferator activated receptor γ.

the TGF-β1/SMAD3 signaling pathway in PQ-induced pulmonary fibrosis.

5-ASA is an anti-inflammatory agent commonly used in the treatment of IBD (40). Although the exact mechanisms of action of 5-ASA have not yet been completely elucidated, recent studies have revealed that the basic mechanism of action of 5-ASA relies on increased expression of PPARγ (21,41). As a ligand of PPAR, 5-ASA can increase PPARγ expression, promote its translocation from the cytoplasm to the nucleus and induce activation of the downstream signaling pathway (18,20).

The results of the current study showed that 5-ASA treatment significantly relieved PQ-induced pulmonary fibrotic changes in rats. To explore the putative mechanism of the attenuating effects of 5-ASA on PQ-induced pulmonary fibrotic changes, the expression and interaction of TGF-β1/SMAD3 signaling and PPARγ were studied both *in vivo* in rats and *in vitro* in human lung fibroblasts. The results showed that 5-ASA treatment significantly prevented the upregulation of TGF-β1, the phosphorylation level of SMAD3 and the downregulation of PPARγ induced by PQ in human lung fibroblasts. Collectively, these data suggested that 5-ASA treatment could attenuate PQ-induced pulmonary fibrosis progression by upregulating the expression of PPARγ and inhibiting the TGF-β1/SMAD3 signaling pathway.

In conclusion, to the best of our knowledge, this study showed for the first time that 5-ASA had significant inhibitory effects on pulmonary fibrosis progression in a PQ intoxication rat model, and these effects may be partly ascribed to the inhibition of the TGF-β1/SMAD3 signaling pathway. Thus, 5-ASA may have potential value in the treatment of PQ-induced pulmonary fibrosis.

Acknowledgements

Not applicable.

Funding

This work was supported by the Natural Science Foundation of China (grant no. 81672706).

Availability of data and materials

The datasets used and/or analyzed during the current study are available from the corresponding author on reasonable request.

Authors' contributions

HC and JC conducted the experiments and wrote the manuscript. JW, YW, FT, YT, YG, YM and LL collected the data and performed the experiments and XZ designed the study. HC and XZ confirm the authenticity of all the raw data. All authors have read and approved the final manuscript.

Ethics approval and consent to participate

All experiments were performed in compliance with the Guide for the Care and Use of Laboratory Animals of the National Institutes of Health (NIH Publication No. 8023, Revised 1978) and were reviewed and approved by the Ethics Committee for the Use of Experimental Animals at Hebei Medical University (approval no. 1608303; Shijiazhuang, China).

Patient consent for publication

Not applicable.

Competing interests

The authors declare that they have no competing interests.

References

1. Sun B and Chen YG: Advances in the mechanism of paraquat-induced pulmonary injury. Eur Rev Med Pharmacol Sci 20: 1597-1602, 2016.
2. Zhou Q, Kan B, Jian X, Zhang W, Liu H and Zhang Z: Paraquat poisoning by skin absorption: Two case reports and a literature review. Exp Ther Med 6: 1504-1506, 2013.
3. Kimbrough RD and Linder RE: The ultrastructure of the paraquat lung lesion in the rat. Environ Res 6: 265-273, 1973.
4. Shadnia S, Ebadollahi-Natanzi A, Ahmadzadeh S, Karami-Mohajeri S, Pourshojaei Y and Rahimi HR: Delayed death following paraquat poisoning: Three case reports and a literature review. Toxicol Res (Camb) 7: 745-753, 2018.
5. Tsoyi K, Chu SG, Patino-Jaramillo NG, Wilder J, Villalba J, Doyle-Eisele M, McDonald J, Liu X, El-Chemaly S, Perrella MA and Rosas IO: Syndecan-2 Attenuates Radiation-induced pulmonary fibrosis and inhibits fibroblast activation by regulating PI3K/Akt/ROCK Pathway via CD148. Am J Respir Cell Mol Biol 58: 208-215, 2018.
6. Kan B, Jian X, Zhou Q, Wang J, Yu G, Sun J and Gao Y: Effect of transforming growth factor-beta1 on acute lung injury caused by paraquat. Mol Med Rep 9: 1232-1236, 2014.
7. Han YY, Shen P and Chang WX: Involvement of epithelial-to-mesenchymal transition and associated transforming growth factor-β/Smad signaling in paraquat-induced pulmonary fibrosis. Mol Med Rep 12: 7979-7984, 2015.
8. Hua XF, Li XH, Li MM, Zhang CY, Liu HJ, Sun T, Zhou HG and Yang C: Doxycycline attenuates paraquat-induced pulmonary fibrosis by downregulating the TGF-β signaling pathway. J Thorac Dis 9: 4376-4386, 2017.
9. Ren Y, Jian X, Zhang Z, Ning Q, Kan B and Kong L: Effects of tacrolimus on the TGF-β1/SMAD signaling pathway in paraquat-exposed rat alveolar type II epithelial cells. Mol Med Rep 22: 3687-3694, 2020.
10. Hu Z, Qin F, Gao S, Zhen Y, Huang D and Dong L: Paeoniflorin exerts protective effect on radiation-induced hepatic fibrosis in rats via TGF-β1/Smads signaling pathway. Am J Transl Res 10: 1012-1021, 2018. eCollection 2018.
11. Sato M, Muragaki Y, Saika S, Roberts AB and Ooshima A: Targeted disruption of TGF-beta1/Smad3 signaling protects against renal tubulointerstitial fibrosis induced by unilateral ureteral obstruction. J Clin Invest 112: 1486-1494, 2003.
12. Loboda A, Sobczak M, Jozkowicz A and Dulak J: TGF-β1/Smads and miR-21 in renal fibrosis and inflammation. Mediators Inflamm 2016: 8319283, 2016.
13. Sisto M, Lorusso L, Ingravallo G, Tamma R, Ribatti D and Lisi S: The TGF-β1 signaling pathway as an attractive target in the fibrosis pathogenesis of Sjogren's Syndrome. Mediators Inflamm 2018: 1965935, 2018.
14. Ramirez A, Ballard EN and Roman J: TGFβ1 Controls PPARγ expression, transcriptional potential, and activity, in part, through Smad3 Signaling in Murine lung fibroblasts. PPAR Res 2012: 375876, 2012.
15. Calvier L, Chouvarine P, Legchenko E, Hoffmann N, Geldner J, Borchert P, Jonigk D, Mozes MM and Hansmann G: PPARγ Links BMP2 and TGFβ1 pathways in vascular smooth muscle cells, regulating cell proliferation and glucose metabolism. Cell Metab 25: 1118-1134.e7, 2017.
16. Solitano V, D'Amico F, Fiorino G, Paridaens K, Peyrin-Biroulet L and Danese S: Key strategies to optimize outcomes in Mild-to-Moderate Ulcerative Colitis. J Clin Med 9: 2905, 2020.
17. Le Berre C, Roda G, Nedeljkovic Protic M, Danese S and Peyrin-Biroulet L: Modern use of 5-aminosalicylic acid compounds for ulcerative colitis. Expert Opin Biol Ther 20: 363-378, 2020.
18. Cevallos SA, Lee JY, Velazquez EM, Foegeding NJ, Shelton CD, Tiffany CR, Parry BH, Stull-Lane AR, Olsan EE, Savage HP, *et al*: 5-Aminosalicylic Acid Ameliorates Colitis and checks Dysbiotic Escherichia coli expansion by activating PPAR-γ Signaling in the intestinal epithelium. mBio 12: e03227-20, 2021.
19. Vetuschi A, Pompili S, Gaudio E, Latella G and Sferra R: PPAR-γ with its anti-inflammatory and anti-fibrotic action could be an effective therapeutic target in IBD. Eur Rev Med Pharmacol Sci 22: 8839-8848, 2018.
20. Rousseaux C, El-Jamal N, Fumery M, Dubuquoy C, Romano O, Chatelain D, Langlois A, Bertin B, Buob D, Colombel JF, *et al*: The 5-aminosalicylic acid antineoplastic effect in the intestine is mediated by PPARγ. Carcinogenesis 34: 2580-2586, 2013.

21. Wang Z, Koonen D, Hofker M and Bao Z: 5-aminosalicylic acid improves lipid profile in mice fed a high-fat cholesterol diet through its dual effects on intestinal PPARgamma and PPARalpha. PLoS One 13: e0191485, 2018.
22. Wang Y, Zhou M, Lu Y, Yu A and Li J: Protective effect of 5-aminosalicylic acid on the kidney of paraquat poisoning rats by Nrf2-ARE signal pathway. Zhonghua Wei Zhong Bing Ji Jiu Yi Xue 29: 961-966, 2017 (In Chinese).
23. Ramadan A, Afifi N, Yassin NZ, Abdel-Rahman RF, Abd El-Rahman SS and Fayed HM: Mesalazine, an osteopontin inhibitor: The potential prophylactic and remedial roles in induced liver fibrosis in rats. Chem Biol Interact 289: 109-118, 2018.
24. Hoffmann M, Kant TA, Emig R, Rausch JSE, Newe M, Schubert M, Künzel K, Winter L, Klapproth E, Peyronnet R, *et al*: Repurposing mesalazine against cardiac fibrosis in vitro. Naunyn Schmiedebergs Arch Pharmacol 394: 533-543, 2021.
25. Schaeffer WI: Proposed usage of animal tissue culture terms (revised 1978). Usage of vertebrate cell, tissue and organ culture terminology. In Vitro 15: 649-653, 1979.
26. Zheng L, Zhang YL, Dai YC, Chen X, Chen DL, Dai YT and Tang ZP: Jianpi Qingchang decoction alleviates ulcerative colitis by inhibiting nuclear factor-KB activation. World J Gastroenterol 23: 1180-1188, 2017.
27. Tang H, Xiang D, Wang F, Mao J, Tan X and Wang Y: 5-ASA-loaded SiO2 nanoparticles-a novel drug delivery system targeting therapy on ulcerative colitis in mice. Mol Med Rep 15: 1117-1122, 2017.
28. Szapiel SV, Elson NA, Fulmer JD, Hunninghake GW and Crystal RG: Bleomycin-induced interstitial pulmonary disease in the nude, athymic mouse. Am Rev Respir Dis 120: 893-899, 1979.
29. Wei J, Ghosh AK, Sargent JL, Komura K, Wu M, Huang QQ, Jain M, Whitfield ML, Feghali-Bostwick C and Varga J: PPARγ downregulation by TGFβ in fibroblast and impaired expression and function in systemic sclerosis: A novel mechanism for progressive fibrogenesis. PLoS One 5: e13778, 2010.
30. Zhang Z, Ding L, Wu L, Xu L, Zheng L and Huang X: Salidroside alleviates paraquat-induced rat acute lung injury by repressing TGF-β1 expression. Int J Clin Exp Pathol 7: 8841-8847, 2014. eCollection 2014.
31. Srivastava AK, Khare P, Nagar HK, Raghuwanshi N and Srivastava R: Hydroxyproline: A potential biochemical marker and its role in the pathogenesis of different diseases. Curr Protein Pept Sci 17: 596-602, 2016.
32. Kuhn C and McDonald JA: The roles of the myofibroblast in idiopathic pulmonary fibrosis. Ultrastructural and immunohistochemical features of sites of active extracellular matrix synthesis. Am J Pathol 138: 1257-1265, 1991.
33. Pache JC, Christakos PG, Gannon DE, Mitchell JJ, Low RB and Leslie KO: Myofibroblasts in diffuse alveolar damage of the lung. Mod Pathol 11: 1064-1070, 1998.
34. Dong J, Yu X, Porter DW, Battelli LA, Kashon ML and Ma Q: Common and distinct mechanisms of induced pulmonary fibrosis by particulate and soluble chemical fibrogenic agents. Arch Toxicol 90: 385-402, 2016.
35. Zhou H, Yu X and Zhou G: NLRC5 silencing ameliorates cardiac fibrosis by inhibiting the TGF-β1/Smad3 signaling pathway. Mol Med Rep 16: 3551-3556, 2017.
36. Xue L, Zhang X, Li Y, Yang H, Li X, Mi J, Wang H, Wang J and Yan X: Differences of immunophenotypic markers and signaling molecules between adenocarcinomas of gastric cardia and distal stomach. Hum Pathol 42: 594-601, 2011.
37. Liu Y, Wang J, Luo S, Zhan Y and Lu Q: The roles of PPARγ and its agonists in autoimmune diseases: A comprehensive review. J Autoimmun 113: 102510, 2020.
38. Carvalho MV, Goncalves-de-Albuquerque CF and Silva AR: PPAR Gamma: From definition to molecular targets and therapy of lung diseases. Int J Mol Sci 22: 805, 2021.
39. Kulkarni AA, Thatcher TH, Olsen KC, Maggirwar SB, Phipps RP and Sime PJ: PPAR-γ ligands repress TGFβ-induced myofibroblast differentiation by targeting the PI3K/Akt pathway: Implications for therapy of fibrosis. PLoS One 6: e15909, 2011.
40. Moran CJ, Huang H, Rivas M, Kaplan JL, Daly MJ and Winter HS: Genetic variants in cellular transport do not affect mesalamine response in ulcerative colitis. PLoS One 13: e0192806, 2018.
41. Serra D, Almeida LM and Dinis TC: Anti-inflammatory protection afforded by cyanidin-3-glucoside and resveratrol in human intestinal cells via Nrf2 and PPAR-γ: Comparison with 5-aminosalicylic acid. Chem Biol Interact 260: 102-109, 2016.